Transport in Porous Media **11:** 243–262, 1993.

On the Use of Conventional Cocurrent and Countercurrent Effective Permeabilities to Estimate the Four Generalized Permeability Coefficients which Arise in Coupled, Two-Phase Flow

RAMON G. BENTSEN
University of Alberta, Department of Mining, Metallurgical and Petroleum Engineering, Edmonton, Alberta, Canada T6G 2G6

and

ABDALLA A. MANAI
Apex Energy Consultants, Calgary, Alberta, Canada T2P 3P2

(Received: 13 June 1991; revised: 2 April 1992)

Abstract. In the case of coupled, two-phase flow of fluids in porous media, the governing equations show that there are four independent generalized permeability coefficients which have to be measured separately. In order to specify these four coefficients at a specific saturation, it is necessary to conduct two types of flow experiments. The two types of flow experiments used in this study are cocurrent and countercurrent, steady-state permeability experiments. It is shown that, by taking this approach, it is possible to define the four generalized permeability coefficients in terms of the conventional cocurrent and countercurrent effective permeabilities for each phase. It is demonstrated that a given generalized phase permeability falls about midway between the conventional, cocurrent effective permeability for that phase, and that for the countercurrent flow of the same phase. Moreover, it is suggested that the conventional effective permeability for a given phase can be interpreted as arising out of the effects of two types of viscous drag: that due to the flow of a given phase over the solid surfaces in the porous medium and that due to momentum transfer across the phase 1-phase 2 interfaces in the porous medium. The magnitude of the viscous coupling is significant, contributing at least 15% to the total conventional cocurrent effective permeability for both phases. Finally, it is shown that the nontraditional generalized permeabilities which arise out of viscous coupling effects cannot equal one another, even when the viscosity ratio is unity and the surface tension is zero.

Key words. Countercurrent flow, effective permeability, generalized permeability, viscous coupling

Nomenclature

Roman Letters

$\mathbf{g}$	gravity vector, m^2/s
g_i	function defined by Equation (23)
g_{ij}	functions defined by Equations (19) to (22)
k	absolute permeability, m^2
k_i	effective permeability of phase i; $i = 1, 2$, m^2
k_{ij}	coefficient of generalized permeability for phase i; $i, j = 1, 2$, m^2
k_{rij}	coefficient of generalized relative permeability for phase i; $i, j = 1, 2$
k_{ro}	relative permeability to oil
k_{rw}	relative permeability to water

k_{vi} coefficient of viscous coupling for phase i; $i = 1, 2$, m^2
L length of core, m
P_c capillary pressure, N/m^2
p_i pressure in phase i; $i = 1, 2$, N/m^2
Δp_i pressure drop for phase i; $i = 1, 2$, N/m^2
q_i Darcy flow velocity for phase i; $i = 1, 2$, m/s
R_{12} ratio of pressure gradients (phase 1/phase 2)
S $\dfrac{S_w - S_{wi}}{1 - S_{or} - S_{wi}}$ = normalized saturation
S_{or} residual oil saturation
S_w water saturation
S_{wi} irreducible water saturation

Greek Letters

α interfacial tension, N/m
η_i fraction of pore space occupied by phase i; $i = 1,2$
μ_i viscosity of phase i; $i = 1, 2$, Pa/s
ρ_i density of phase i; $i = 1, 2$, kg/m^3

Subscripts and Superscripts

1 wetting phase
2 nonwetting phase
* countercurrent flow

1. Introduction

Several authors (de la Cruz and Spanos, 1983; Whitaker, 1986; Kalaydjian, 1987) have undertaken a volume averaging of the Navier–Stokes equation to arrive at the governing equations for coupled, immiscible, two-phase flow in porous media. These equations show that four independent generalized permeability coefficients are required to define completely the flow characteristics of a particular porous medium-fluid system. While standard methods for estimating conventional permeabilities are available, laboratory procedures for estimating each of the four generalized permeability coefficients are still under development. Whitaker (1986) has shown that traditional schemes for measuring permeability, i.e. those which are constrained to steady, uniform flows without gravitational effects, do not yield sufficient information to determine uniquely the four generalized permeability coefficients. Rose (1988) has demonstrated that two types of experiments, each type involving two measurements, are needed to provide sufficient information to determine uniquely the four coefficients at a given saturation. Moreover, he has suggested that two steady-state, uniform-flow experiments, one with gravitational effects and one without, be used to determine the four coefficients. However, in a later paper, Rose (1989) presented an error analysis which indicated that, if this approach were to be used, measurement errors would be expected to have an enormous impact on the accuracy of the calculated generalized permeabilities, even if valid procedures for practical cases were rigorously followed. Kalaydjian (1990) has suggested also that two experiments are required to measure the four coefficients. Moreover, he has proposed that the first one be a cocurrent displacement without any capillary effect and that the second one be a countercurrent-flow experiment (with zero total flow).

If one is to determine the four generalized permeability coefficients, it seems clear that two separate experiments must be undertaken. Moreover, because steady-state permeability experiments involve direct measurement of variables, and because they involve fewer assumptions than do unsteady-state permeability experiments, it seems advisable that the two experiments be steady-state, uniform-flow experiments. Hence, one of the experiments can be the traditional steady-state experiment for

determining effective permeabilities under conditions of cocurrent flow. Based on the error analysis undertaken by Rose (1989), it does not appear to be practicable to attempt the traditional steady-state flow experiment, modified to include gravitational effects, as the second experiment. Consequently, another approach must be found. One possibility is to make the second experiment a horizontal, countercurrent-flow, steady-state experiment. While such an experiment, to the best of the authors' knowledge, has never been reported in the literature, a recent study (Bentsen and Manai, 1992) has indicated that this may be a practical way to acquire the additional information needed to determine uniquely the four generalized permeability coefficients.

2. Equations for Determining Generalized Coefficients

Using volume averaging, de la Cruz and Spanos (1983) have shown that the generalized equations for the flow of two continuous phases through a homogeneous, isotropic porous medium are

$$\mu_1\left[\frac{1}{k_{11}}\mathbf{q}_1 - \frac{1}{k_{12}}\mathbf{q}_2\right] = -\nabla p_1 + \rho_1 \mathbf{g} \tag{1}$$

and

$$\mu_2\left[\frac{1}{k_{22}}\mathbf{q}_2 - \frac{1}{k_{21}}\mathbf{q}_1\right] = -\nabla p_2 + \rho_2 \mathbf{g}, \tag{2}$$

where k_{11} and k_{22} are the generalized phase permeabilities for phases 1 and 2, respectively, and where k_{12} and k_{21} are the viscous drag coefficients which represent the viscous drag that exists between phases 1 and 2.

For a horizontal, one-dimensional system in which uniform, steady-state, concurrent flow is taking place, Equations (1) and (2) may be rewritten as

$$\mu_1\left[\frac{1}{k_{11}}q_1 - \frac{1}{k_{12}}q_2\right] = -\frac{\Delta p_1}{L} \tag{3}$$

and

$$\mu_2\left[\frac{1}{k_{22}}q_2 - \frac{1}{k_{21}}q_1\right] = -\frac{\Delta p_2}{L}. \tag{4}$$

If the quantities measured in a countercurrent, steady-state flow experiment are designated by an asterisk (*), and if it is assumed that pressure is distributed linearly in countercurrent, as well as cocurrent, steady-state flow, then the equations for a countercurrent-flow experiment become, in view of Equations (3) and (4),

$$\mu_1\left[\frac{1}{k_{11}}q_1^* - \frac{1}{k_{12}}q_2^*\right] = -\frac{\Delta p_1^*}{L} \tag{5}$$

and

$$\mu_2\left[\frac{1}{k_{22}}q_2^* - \frac{1}{k_{21}}q_1^*\right] = -\frac{\Delta p_2^*}{L}. \tag{6}$$

Equations (3) through (6) constitute a system of equations involving four unknowns, the generalized permeability coefficients k_{11}, k_{12}, k_{22}, and k_{21}. This system of equations may be solved for these coefficients to yield

$$k_{11} = \frac{\dfrac{q_1}{q_2} - \dfrac{q_1^*}{q_2^*}}{\dfrac{1}{\mu_1}\left[\dfrac{1}{q_2^*}\dfrac{\Delta p_1^*}{L} - \dfrac{1}{q_2}\dfrac{\Delta p_1}{L}\right]}, \tag{7}$$

$$k_{12} = \frac{\dfrac{q_2^*}{q_1^*} - \dfrac{q_2}{q_1}}{\dfrac{1}{\mu_1}\left[\dfrac{1}{q_1^*}\dfrac{\Delta p_1^*}{L} - \dfrac{1}{q_1}\dfrac{\Delta p_1}{L}\right]}, \tag{8}$$

$$k_{22} = \frac{\dfrac{q_2}{q_1} - \dfrac{q_2^*}{q_1^*}}{\dfrac{1}{\mu_2}\left[\dfrac{1}{q_1^*}\dfrac{\Delta p_2^*}{L} - \dfrac{1}{q_1}\dfrac{\Delta p_2}{L}\right]}, \tag{9}$$

and

$$k_{21} = \frac{\dfrac{q_1^*}{q_2^*} - \dfrac{q_1}{q_2}}{\dfrac{1}{\mu_2}\left[\dfrac{1}{q_2^*}\dfrac{\Delta p_2^*}{L} - \dfrac{1}{q_2}\dfrac{\Delta p_2}{L}\right]}. \tag{10}$$

For experimental reasons, it is not possible to ensure that a cocurrent, and its associated countercurrent, flow experiment are conducted at exactly the same saturation. As a consequence, it is necessary to correlate the measured ratios of flow rates and pressure gradients against saturation. It is convenient, and understandable, to use the conventional two-phase flow equations for this purpose. The conventional steady-state equations for cocurrent flow may be written as

$$q_1 = -\frac{k_1}{\mu_1}\frac{\Delta p_1}{L} \tag{11}$$

and

$$q_2 = -\frac{k_2}{\mu_2}\frac{\Delta p_2}{L}, \tag{12}$$

while those for countercurrent flow may be written as

$$q_1^* = -\frac{k_1^*}{\mu_1}\frac{\Delta p_1^*}{L} \tag{13}$$

and

$$q_2^* = -\frac{k_2^*}{\mu_2}\frac{\Delta p_2^*}{L}. \tag{14}$$

If Equations (11) through (14) are introduced into Equations (7) through (10), it may be shown, after some manipulation, that

$$k_{11} = g_{11}k_1, \tag{15}$$

$$k_{12} = \frac{\mu_1}{\mu_2}g_{12}k_2, \tag{16}$$

$$k_{22} = g_{22}k_2 \tag{17}$$

and

$$k_{21} = \frac{\mu_2}{\mu_1}g_{21}k_1, \tag{18}$$

where

$$g_{11} = \frac{g_1}{R_{12}^* + R_{12}\dfrac{k_2^*}{k_2}}, \tag{19}$$

$$g_{12} = \frac{1}{R_{12} + R_{12}^*}\frac{g_1}{1 - \dfrac{k_1^*}{k_1}}, \tag{20}$$

$$g_{22} = \frac{g_1}{R_{12}^*\dfrac{k_1^*}{k_1} + R_{12}}, \tag{21}$$

$$g_{21} = \frac{g_1}{1 - \dfrac{k_2^*}{k_2}}, \tag{22}$$

$$g_1 = R_{12}^*\frac{k_1^*}{k_1} + R_{12}\frac{k_2^*}{k_2}, \tag{23}$$

$$R_{12} = \frac{\Delta p_1}{\Delta p_2} \tag{24}$$

and

$$R_{12}^* = -\frac{\Delta p_1^*}{\Delta p_2^*}. \tag{25}$$

Note that, while it is usual to assume that R_{12} is equal to unity (Collins, 1961), there is no experimental basis for assuming that such is the case, as well, for R_{12}^*. In fact, the theoretical analysis of Eastwood and Spanos (1991) suggests that it is not.

3. Equations for Determining the Viscous Coupling Coefficients

Equation (3) may be rearranged to read

$$-\frac{\mu_1 q_1 L}{\Delta p_1} = k_{11} - \mu_1 \frac{k_{11}}{k_{12}} \frac{q_2 L}{\Delta p_1}. \tag{26}$$

If Equations (11), (12), and (24) are introduced into Equation (26), it may be shown that

$$k_1 = k_{11} + \frac{\mu_1}{\mu_2} \frac{k_{11}}{k_{12}} \frac{k_2}{R_{12}}. \tag{27}$$

The generalized permeability coefficient, k_{11}, represents the influence of the viscous drag of fluid 1 on the solid surfaces in the porous medium (Spanos *et al.*, 1988). Moreover, as noted by Whitaker (1986), the ratio k_{11}/k_{12} represents the influence of the viscous drag that exists between phase 1 and phase 2. Thus, in view of Equation (27), one can view the conventional permeability, k_1, as representing the influence of two types of drag within the porous medium: that due to the flow of the fluid itself over the solid surfaces, and that due to momentum transfer across the fluid-fluid interfaces.

By introducing Equations (15) and (16) into Equation (27), it may be demonstrated that

$$k_1 = k_{11} + k_{v1}, \tag{28}$$

where

$$k_{v1} = \frac{k_1 - k_1^*}{1 + \dfrac{R_{12}}{R_{12}^*} \dfrac{k_2^*}{k_2}}. \tag{29}$$

Similarly, it may be shown that

$$k_2 = k_{22} + k_{v2}, \tag{30}$$

where

$$k_{v2} = \frac{k_2 - k_2^*}{1 + \dfrac{R_{12}^*}{R_{12}} \dfrac{k_1^*}{k_1}}. \tag{31}$$

4. Experimental Materials, Equipment and Procedure

4.1 MATERIALS

The coreholder in which the experiments were conducted had a length of 1.00 m, a width of 0.011 m and a height of 0.0565 m. The unconsolidated porous media used in this study were prepared by wet-packing the coreholder with Ottawa sand (70–30 mesh sieved to obtain 80–120 mesh). For each run, the sandpack was dried, evacuated, and then resaturated with distilled water in order to be able to measure the porosity and absolute permeability of the sandpack. This method of packing the coreholder yielded sandpacks having porosities of about 0.35 and absolute permeabilities of about 20 μm^2. Distilled water was used as the wetting fluid (fluid 1) and MCT-5, a refined oil supplied by Imperial Oil Limited, was used as the nonwetting fluid (fluid 2). The use of these fluids resulted in a viscosity ratio, μ_2/μ_1, of about 30.

4.2. EQUIPMENT

The experimental apparatus used in this study is essentially similar to that reported elsewhere (Sarma and Bentsen, 1989a; Sarma and Bentsen, 1989b; Sarma and Bentsen, 1990). Data from the pressure transducers mounted on the coreholder were recorded automatically by a data acquisition system. Moreover, a comprehensive interactive software routine was used which enabled almost complete automation of the experimental runs. The Ruska pumps used to inject the wetting and nonwetting phases at a constant rate were the only units not controlled by the data acquisition system.

The coreholder used in this study has fourteen pressure transducer taps, seven located on the top and seven located on the bottom of the coreholder. Fritted discs wetted by oil, the nonwetting phase, were mounted in the pressure transducer taps located on the top of the coreholder, while fritted discs wetted by water, the wetting phase, were mounted in those located on the bottom of the coreholder. Consequently, it was possible to measure directly the pressure in both the wetting and nonwetting phases at given positions along the length of the core. Further details with respect to how the pressures were measured are available elsewhere (Manai, 1991; Bentsen and Manai, 1991).

Saturations were measured *in situ* using the microwave method. The microwave instrumentation used was similar to that employed on earlier related studies (Sarma and Bentsen, 1989a; Sarma and Bentsen, 1989b; Sarma and Bentsen, 1990). The reader interested in specific details on how the saturations were measured in this study is referred to Sarma and Bentsen, 1990 and Manai, 1991.

4.3. EXPERIMENTAL PROCEDURE

The following procedure was used in each of the steady-state relative permeability experiments. First, in order to establish an irreducible water saturation, the resident

water was displaced by injecting MCT-5 until such time as the incremental recovery of water became essentially zero. This normally required the injection of about four pore volumes of oil. During this part of the procedure, the pressure transducer taps were fitted with dummy plugs. Once the irreducible water saturation had been achieved, the effective permeability to oil of the system was determined. This was accomplished by replacing two of the dummy plugs, one at the inlet and one at the outlet end, with fritted discs wetted by oil and pressure transducers, so that the total pressure drop across the core could be determined. Next, the remaining dummy plugs were removed so that the fritted discs wetted by water (or oil) and the pressure transducers could be installed in the remaining taps. Then the preparation end caps were replaced by the cocurrent-flow end caps, each of which contained two plates with an opening in each plate. One of these plates was wetted by water and the other by oil.

All experiments began with the core at irreducible water saturation. For the cocurrent-flow experiments, both fluids were injected, at various fixed ratios, into the core in the same direction, with the oil being injected through the oil-wet plate and the water through the water-wet plate. The injection rates for water varied between 7.5 and 200 ml/h, while those for oil varied between 2.0 and 40 ml/h. Such injection was continued for a period of time sufficient to ensure that steady state was achieved. Usually injection was continued for the maximal permissible time, which was dictated by the capacities of the Ruska pump cylinders and the respective rates at which the fluids were being injected.

During the experiment, the core was scanned periodically by microwaves to determine how saturation was distributed along the length of the core. Moreover, pressure readings were taken at the same time the core was scanned. The interval between microwave scans was selected on the basis of the injection rate and the duration of the run. This enabled scanning of the core at regular time intervals. A scan was achieved by drawing the coreholder between two fixed microwave antennas.

For each ratio of flow rates, the data were analyzed, and only the portion of the data set for which steady state had been achieved was retained for further analysis. To minimize boundary effects, calculations were made as if the core were only 96 cm long. That is, only the length of core between the two far transducers (each of which was located 2 cm from the end of the coreholder) was considered in the analysis. Effective permeabilities for both oil and water at a specific saturation were determined using the appropriate form of Darcy's law, and relative permeabilities were then obtained as ratios between the effective permeabilities and the absolute permeability of the core. Then the ratio of flow rates was changed, and the experiment was repeated until a complete set of imbibition relative permeability data was obtained.

After the cocurrent-flow relative permeabilities had been obtained, the coccurent-flow end caps of the coreholder were replaced with preparation end caps. The core

was then reflooded with oil until the irreducible water saturation was reestablished. This was accomplished by continuing the oilflood until the volume of water remaining in the core was, within experimental error, the same as that obtained in the cocurrent experiments. The pressure transducers were then recalibrated to ensure accurate pressure measurement.

Once the irreducible water saturation had been reestablished, the countercurrent-flow end caps were installed and a microwave scan was performed to determine the irreducible water saturation. After choosing a flow-rate ratio, oil was injected into one end of the coreholder and water into the other. The injection rates for water varied between 2.0 and 120 ml/h, while those for oil varied between 2.0 and 35 ml/h. As in the cocurrent experiments, microwave scans and pressure measurements were performed regularly throughout the experiment. Once steady state had been achieved, the effective and relative permeabilities were determined. Then the ratio of flow rates was changed and the experiment repeated until another complete set of imbibition relative permeability data was obtained.

6. Results

In order to evaluate the proposed method for determining the generalized permeability coefficients, two sets of steady-state permeability experiments were undertaken, the second set being a replicate of the first. *In situ* measurements were made to ascertain how saturation and pressure (in both phases) were distributed along the core. As can be seen from Figures 1 and 2, it was found for both cocurrent (Figure 1) and countercurrent flow (Figure 2), that saturation was invariant with distance, once steady-state flow was attained. Moreover, as can be seen from Figures 3 and 4, the pressure in both phases was distributed linearly with distance for both cocurrent flow

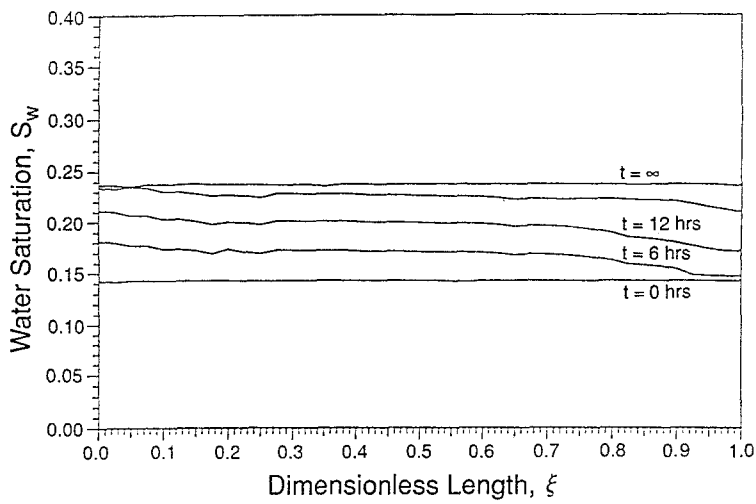

Fig. 1. Typical dynamic water saturation profiles during cocurrent flow.

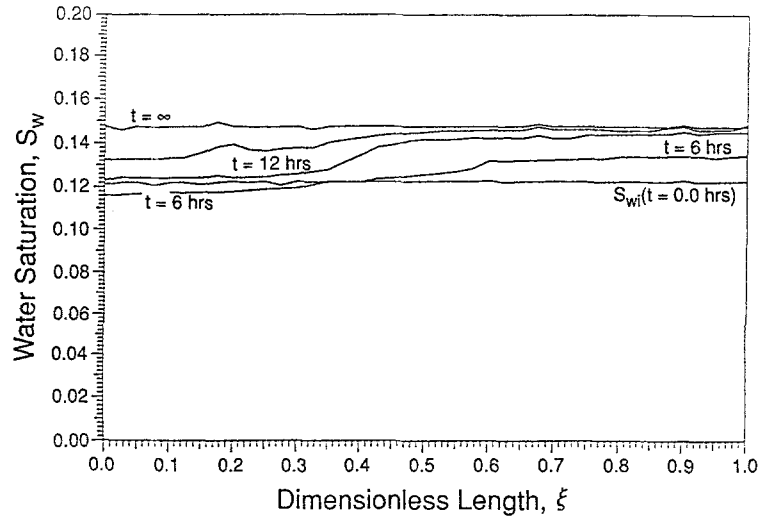

Fig. 2. Typical dynamic water saturation profiles during countercurrent flow.

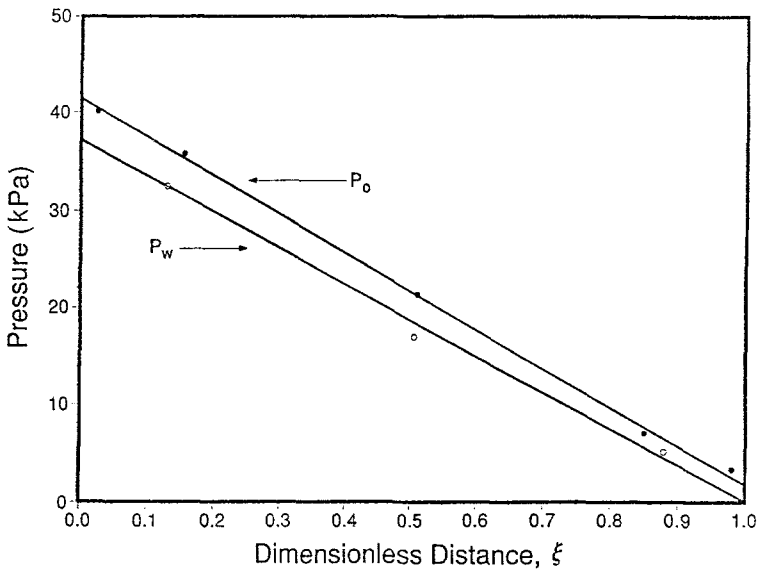

Fig. 3. Typical pressure profiles during cocurrent flow.

(Figure 3) and countercurrent flow (Figure 4), once stabilization of the flow was achieved. Except where noted, the results obtained from the replicate set of data were essentially similar to those obtained using the first set of data. Further details with respect to this aspect of the experiments are available elsewhere (Manai, 1991; Bentsen and Manai, 1991).

Relative permeabilities were constructed by dividing the effective permeabilities obtained in the flow experiments by the absolute permeability of the sand pack. Relative permeability curves obtained in this way for Data Set 1 are depicted in Figure 5,

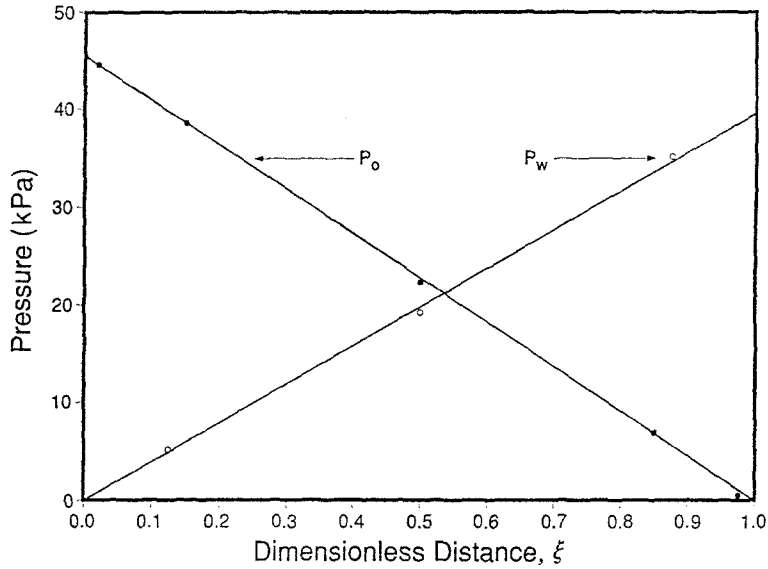

Fig. 4. Typical pressure profiles during countercurrent flow.

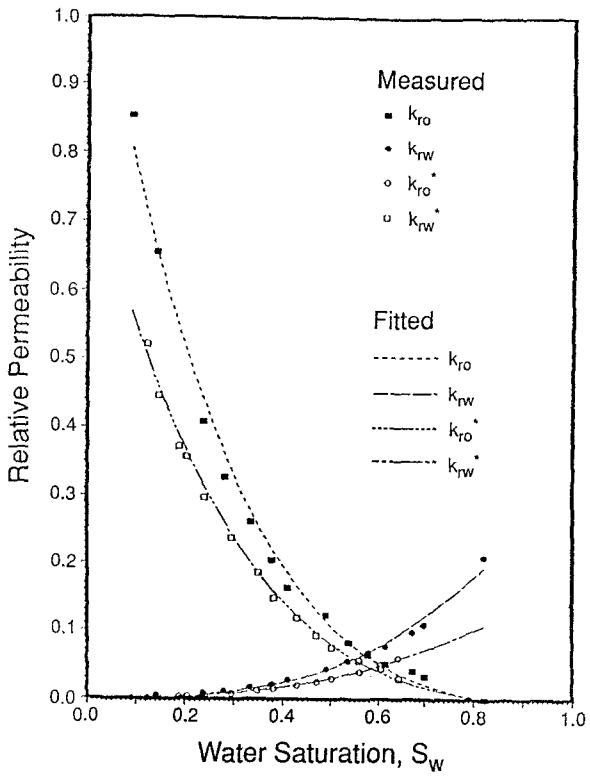

Fig. 5. Comparison of measured and fitted relative permeabilities for cocurrent and countercurrent flow (Set I).

where the upper curves are those determined for cocurrent flow, and the lower curves are those determined for countercurrent flow.

In order to determine the generalized permeability curves, it is necessary to know the relationship between R_{12} and R_{12}^* and saturation. How R_{12} and R_{12}^* varied with normalized saturation for Data Set 1 is presented in Figure 6.

As noted earlier, it was not possible to ensure that a cocurrent-flow experiment and its associated countercurrent-flow experiment were conducted at the same saturation. Consequently, it was necessary to fit both the effective permeability and pressure-ratio data. These fitted curves, together with Equations (15) and (17), were used to estimate k_{11} and k_{22}. Then these curves were divided by k to obtain k_{r11} and k_{r22}. A comparison of k_{r11} and k_{r22} with the cocurrent and countercurrent relative permeability curves for Data Set 1 is depicted in Figure 7. Notice that k_{r11} and k_{r22} appear to fall approximately midway between the associated cocurrent and countercurrent relative permeability curves.

The relative viscous drag coefficients, k_{r12} and k_{r21}, were constructed by dividing k_{12} and k_{21}, by k. How k_{r12} nd k_{r21} varied with saturation for Data Set 1 is shown in Figure 8. The k_{r12} curve obtained from the replicate set of data was essentially similar to the one shown in Figure 8. However, the k_{r21} curve was not. For the replicate data set, the k_{r21} curve attained a maximal value of

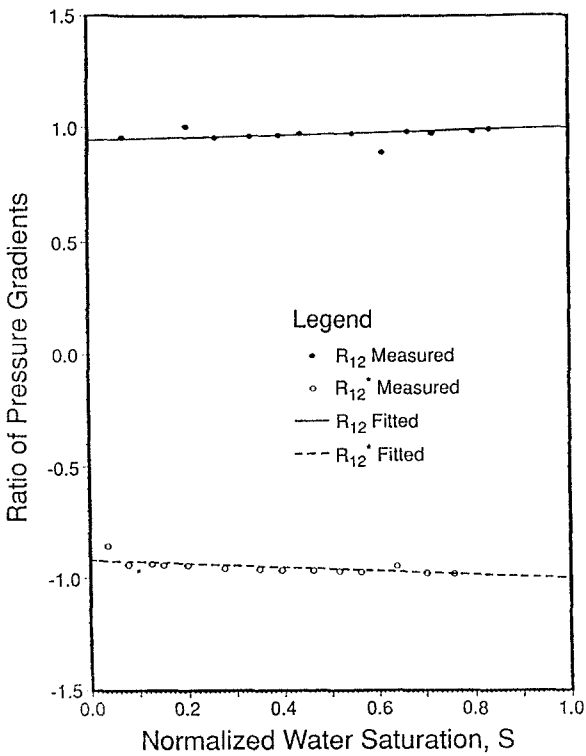

Fig. 6. Ratios of pressure gradients between water and oil for cocurrent and countercurrent flow (Set I).

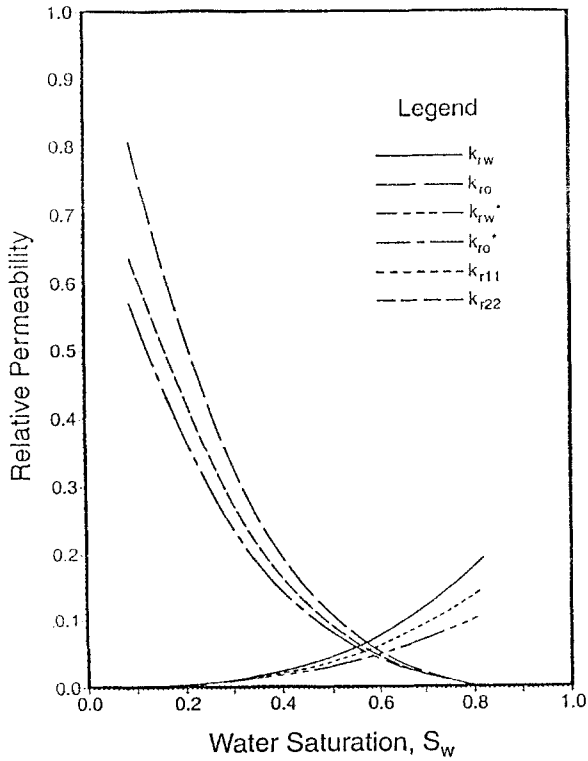

Fig. 7. Comparison of relative permeabilities for cocurrent and countercurrent flow with generalized relative permeabilities (Set I).

approximately 18 at $S_w = 0.70$, and then decreased to a value of approximately 15 at $S_w = 1 - S_{or}$. This difference in behavior between the two curves is attributed to a lack of precision, at high water saturation values, of the measured k_{ro} data (see Figure 5).

The relative viscous coupling coefficients, k_{rv1} and k_{rv2}, as functions of saturation, for Data Set 1 are shown in Figure 9. Note that the maximal amount of momentum transfer across the fluid-fluid interfaces in the porous medium appears to occur at the end-point saturations.

6. Discussion of Results

6.1. RELATIVE PERMEABILITY CURVES

The steady-state cocurrent and countercurrent relative permeability curves obtained in this study (see Figure 5) exhibit the typical shape of water-wet, steady-state relative permeability curves. As can be seen from Figure 5, the relative permeability for countercurrent flow, at a given saturation, is always less than that for cocurrent flow. In particular, the relative difference between the wetting cocurrent-flow relative

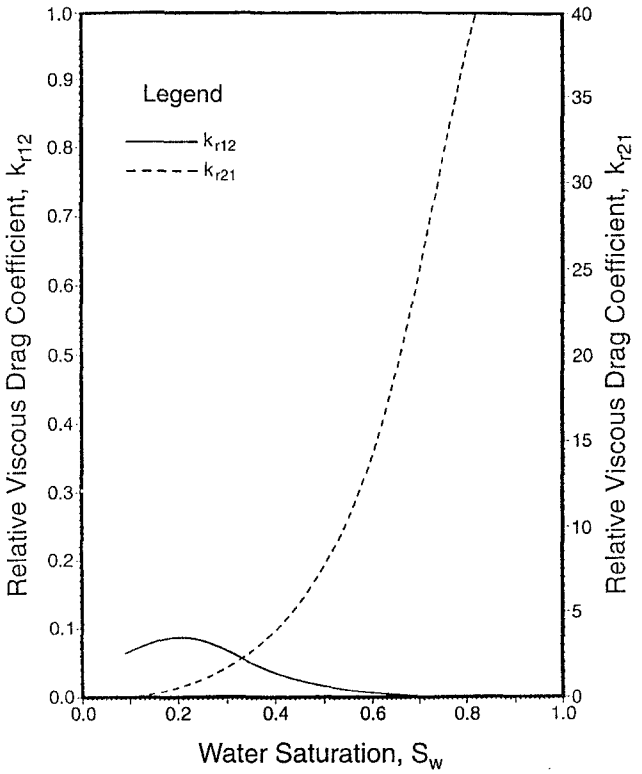

Fig. 8. Relative viscous drag coefficients (Set I).

permeability and that for countercurrent flow was always greater than 25%, while the relative difference between the nonwetting, cocurrent-flow relative permeability and that for countercurrent flow was always greater than 20%. These observations are consistent with those found in earlier experimental studies dealing with countercurrent flow (Lelièvre, 1966; Bourbiaux and Kalaydjian, 1990). Lelièvre (1966) found that the relative difference between cocurrent and countercurrent wetting relative permeabilities was always greater than 25% for wetting-phase saturations less than 50%. For the nonwetting relative permeabilities, he found that the relative difference between the cocurrent and countercurrent relative permeabilities always exceeded 35% for wetting-phase saturations less than 80%. Bourbiaux and Kalaydjian (1990) were able to obtain a good match of their (unsteady-state) experimental results by using countercurrent relative permeabilities which were 30% less than the cocurrent relative permeabilities. Finally, these results are consistent with the theoretical predictions made by Eastwood and Spanos (1991). However, the validity of some aspects of their theoretical analysis is questionable because they predict a saturation gradient in two-phase, countercurrent flow, contrary to what was found in this study (Bentsen and Manai, 1991).

In concurrent flow, the pressure gradients are oriented in the same direction. As a consequence, the displacement of a given liquid phase contributes positively to the

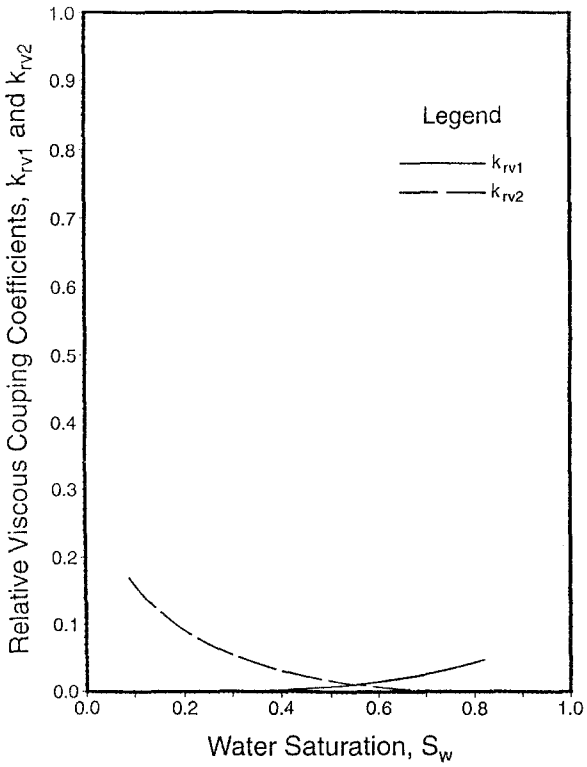

Fig. 9. Relative viscous coupling coefficients (Set I).

flow of the other phase. The result of such viscous coupling, as can be seen in Figure 7, is that k_{rw} and k_{ro} are greater than k_{r11} and k_{r22}, respectively. In countercurrent flow, the pressure gradients act in opposite directions, thereby causing the displacement of one phase to contribute negatively to the flow of the other phase. Consequently, in this case, the effect of the viscous coupling is to cause k^*_{rw} and k^*_{ro} to be less than k_{r11} and k_{r22}, respectively (see Figure 7).

6.2. PRESSURE-GRADIENT RATIO CURVES

The pressures in two immiscible phases which are flowing in a porous medium are not, in general, equal in the plane normal to the direction of flow. This is because, as noted by Leverett (1941), the two phases are separated by curved interfaces. As a reasonable approximation, Leverett assumed that the difference in pressure between the two phases is defined by P_c, the capillary pressure. This assumption enabled Leverett to postulate that the pressure gradients in two-phase, immiscible flow are related by the capillary pressure gradient, a quantity which is dependent upon saturation gradient and saturation only, provided the assumption concerning P_c is valid.

While it is usual to treat Leverett's assumption with respect to capillary pressure as axiomatic (Collins, 1961), some questions have arisen with respect to its validity

under dynamic conditions (see, for example, Rose, 1972). However, the consensus of opinion appears to be that capillary pressure is independent of dynamic effects, provided the capillary number is much smaller than one (Philip, 1972; Wooding and Morel-Seytoux, 1976), as it usually is in practical problems. Some theoretical support is available for this position (Spanos *et al.*, 1986; Whitaker, 1986).

The experimental results obtained in this study do not support the usual contention (Collins, 1961) that, in a steady-state permeability experiment, the pressure gradient in the wetting phase is identical to that in the nonwetting phase, provided saturation is invariant with distance, and provided outlet end effects are avoided. Rather, in the case of cocurrent flow, it was found that the two pressure profiles were only approximately parallel (see Figure 3), while, in the case of countercurrent flow (see Figure 4), the sign of the slope of the nonwetting-phase pressure profile was opposite to that for the wetting-phase pressure profile (Bentsen and Manai, 1991). Moreover, in both types of experiment, the ratio of the pressure gradients, as can be seen in Figure 6, was found to be a weak function of normalized saturation. These results cast doubt on the validity of using the capillary pressure function to define the difference in pressure which exists between two immiscible phases flowing simultaneously through a porous medium, as is usually done. Some theoretical support for this result has been obtained recently (Spanos *et al.*, 1991; Eastwood, 1992).

6.3. RELATIVE VISCOUS DRAG CURVES

The relative viscous drag coefficients, k_{r12} and k_{r21}, are presented in Figure 8. Note that the magnitude of k_{r12} is much less than that of k_{r21}. This is because k_{r12} is proportional to μ_1/μ_2 (see Equation (16)), while k_{r21} is proportional to μ_2/μ_1 (see Equation (18)). This result is consistent with the order of magnitude analysis carried out by Whitaker (1986).

Kalaydjian (1990) suggests that the ratio of the viscous drag coefficients is equal to the viscosity ratio. He justifies his result by invoking Onsager's reciprocity equations, which are valid provided the thermodynamics of irreversible processes is applicable. Spanos *et al.* (1986) use volume averaging of the dynamic Laplace formula to obtain a relationship between the viscous drag coefficients, k_{12} and k_{21}, and interfacial tension, which may be stated as

$$\frac{\mu_2}{k_{21}} - \frac{\mu_1}{k_{12}} = \frac{\alpha f_2}{\eta_1 \eta_2}. \tag{32}$$

Note that, if the interfacial tension, α, is set identically equal to zero in Equation (32), the ratio k_{12}/k_{21} equals μ_1/μ_2.

A relationship between k_{12} and k_{21} can be constructed also by using the results obtained in this study. Thus, if one divides Equation (16) by Equation (18), it can be shown, after some manipulation, that

$$\frac{k_{12}}{k_{21}} = \left(\frac{\mu_1}{\mu_2}\right)^2 \frac{1}{R_{12} R_{12}^*} \frac{k_2 - k_2^*}{k_1 - k_1^*}. \tag{33}$$

Because Equation (33) is defined in terms of empirical relationships for the pressure ratios, R_{12} and R^*_{12}, and for the effective permeabilities, k_1, k^*_1, k_2 and k^*_2, some caution must be exercised when using Equation (33) to draw conclusions concerning the proper relationship between k_{12} and k_{21}.

As can be seen from Figure 8, k_{r12} tends to zero as S_w tends to $1 - S_{or}$, while k_{r21} tends to zero as S_w tends to S_{wi}. As a consequence, the ratio k_{12}/k_{21} varies between infinity and zero, as S_w increases from S_{wi} to $1 - S_{or}$. While such a result is consistent with Equation (33), it is not consistent with Equation (32). Note that this is the case even for very low values of α, given that the cocurrent effective permeabilities k_1 and k_2 remain distinct from the countercurrent effective permeabilities k^*_1 and k^*_2, respectively, and given that k_1, k^*_1, k_2, and k^*_2 become linear functions of saturation at very low values of α, as suggested by Bardon and Longeron (1980).

6.4. RELATIVE VISCOUS COUPLING CURVES

The effective permeability, k_1, can be considered as being made up of two components (see Equation (28)): the generalized permeability coefficient, k_{11}, and the viscous coupling coefficient, k_{v1}. Similarly, k_2 can be considered as being made up of k_{22} and k_{v2}. In this study, the magnitude of the viscous coupling was found to be significant, contributing at least 15% to the cocurrent effective permeability for both phases (Manai, 1991). Moreover, the contribution of viscous coupling appeared to be minimal at intermediate water saturation values, and increased somewhat at both lower and higher values of water saturation.

Considerable controversy exists as to whether effective permeability depends upon viscosity ratio. For example, Odeh (1959) suggests that it does, while Leverett (1939) suggests that it does not. The results obtained in this study cannot be used to resolve this issue. This is because, even though the viscosity ratio does not appear explicitly in the defining equations for the viscous coupling coefficients (see Equations (29) and (31)), it may still affect the shape and magnitude of the effective permeabilities, k_1, k^*_1, k_2, and k^*_2 (Odeh, 1959). Moreover, there exists the possibility that R_{12} and R^*_{12} may depend upon viscosity ratio.

6.5. ACCURACY OF RESULTS

The magnitude and shape of the generalized relative permeability curves presented in Figures 7–9 depend upon the accuracy of the curves fitted to the effective permeability and pressure-ratio data. The estimated mean square errors for the functions used to fit this data are presented in Table I. Similar mean-square errors were found for the set of replicate experiments.

Because R_{12}, R^*_{12}, k^*_1/k_1, and k^*_2/k_2 appear in the denominator of the defining equations for k_{11} and k_{22} as a sum of terms (see Equations (19) and (21)), minor differences in the magnitude and shape of k_1, k^*_1, k_2, and k^*_2 had only a minor effect

Table I. Estimated mean-square errors for fitted equations

Function	Estimated mean-square error
k_{rw}	5.0×10^{-5}
k_{rw}^*	7.6×10^{-7}
k_{ro}	5.7×10^{-5}
k_{ro}^*	1.9×10^{-5}
R_{12}	8.8×10^{-4}
R_{12}^*	5.1×10^{-4}

on the magnitude and shape of k_{r11} and k_{r22}. Consequently, it is thought that the k_{r11} and k_{r22} curves are reasonably accurate, keeping in mind that only two sets of data have been taken at this point.

Much less certanty exists with respect to the accuracy of k_{r12} and k_{r21}, as compared to k_{r11} and k_{r22}. This is because the ratios k_1^*/k_1 and k_2^*/k_2 appear in the denominator of the defining equations for k_{12} and k_{21} in the form of differences (see Equations (20) and (22)), rather than in the form of sums, as was the case for k_{11} and k_{22}. As a consequence, minor differences in the magnitude and shape of k_1, k_1^*, k_2 and k_2^* resulted in significant differences in the magnitude and shape of k_{r12} and k_{r21}. This was a particular problem with respect to k_2 and k_2^*. That is, as noted earlier, there was a significant difference in the behaviour of k_{r21}, as presented in Figure 8, and that determined using the replicate data set. As a consequence, much less confidence can be had in the accuracy of k_{r12} and k_{r21}, as compared to that for k_{r11} and k_{r22}.

7. Conclusions

A method for estimating the four generalized permeability coefficients which arise for coupled, immiscible, two-phase flow in porous media has been proposed. Using this method, two sets of permeability experiments, the second being a replicate of the first, were carried out in unconsolidated porous media. On the basis of the results obtained in this study, it can be said that countercurrent-flow relative permeabilities are less than cocurrent-flow relative permeabilities. Moreover, the difference between cocurrent-flow and countercurrent-flow relative permeability can be attributed to viscous coupling. The magnitude of the viscous coupling is significant, contributing at least 15% to the cocurrent effective permeabilities for both phases. In addition, the results obtained in this study cast doubt on the validity of using the capillary pressure function to define the difference in pressure which exists between two immiscible phases flowing simultaneously through a porous medium. Finally, it does not appear that k_{21} can equal k_{12}, even when the viscosity ratio is unity and the interfacial tension is zero.

Acknowledgements

The authors wish to express their appreciation to the Natural Sciences and Engineering Research Council of Canada for the financial assistance which made this study possible. Moreover, thanks are extended to Imperial Oil Limited for providing the oil used in this study.

References

Bardon, C. and Longeron, D. G., 1980, Influence of very low interfacial tensions on relative permeability, *Soc. Petrol Eng. J.* **20**, 391–401.

Bentsen, R. G. and Manai, A. A., 1991, Measurement of cocurrent and countercurrent relative permeability curves using the steady-state method, *AOSTRA J. Res.* **1**, 169–181.

Bourbiaux, B. J. and Kalaydjian, F. J., 1990, Experimental study of cocurrent and countercurrent flows in natural porous media, *SPERE* **5**, 361–368.

Collins, R. E., 1961, *Flow of Fluids Through Porous Materials*, Reinhold, New York, pp. 139–169.

de la Cruz, V. and Spanos, T. J. T., 1983, Mobilization of oil ganglia, *AIChE J.* **29**(5), 854–858.

Eastwood, J. E., 1992, Thermomechanics of porous media, PhD Thesis, University of Alberta, Canada.

Eastwood, J. E. and Spanos, T. J. T., 1991, Steady-state countercurrent flow in one dimension, *Transport in Porous Media* **6**, 173–182.

Kalaydjian, F., 1987, A macroscopic description of multiphase flow in porous media involving spacetime evolution of fluid/fluid interface, *Transport in Porous Media* **2**, 537–552.

Kalaydjian, F., 1990, Origin and quantification of coupling between relative permeabilities for two-phase flows in porous media, *Transport in Porous Media* **5**, 215–229.

Lelièvre, R. F., 1966, Etude d'écoulements disphasiques permanents à contre-courants en milieu poreux-Comparison avec les écoulements de même sens (in French), PhD thesis, University of Toulouse, France.

Leverett, M. C., 1939, Flow of oil-water mixtures through unconsolidated sands, *Trans.* AIME **132**, 149–171.

Leverett, M. C., 1941, Capillary behavior in porous solids, *Trans.* AIME **142**, 152–169.

Manai, A. A., 1991, The measurement of cocurrent and countercurrent relative permeabilities and their use to estimate generalized relative permeabilities, MSc thesis, University of Alberta.

Odeh, A. S., 1959, Effect of viscosity on relative permeability, *Trans.* AIME **216**, 346–353.

Rose, W., 1988, Measuring transport coefficients necessary for the description of coupled two-phase flow of immiscible fluids in porous media, *Transport in Porous Media* **3**, 163–171.

Rose, W., 1989, Data interpretation problems to be expected in the study of coupled fluid flows in porous media, *Transport in Porous Media* **4**, 185–198.

Rose, W., 1972, Some problems connected with the use of classical description of fuid/fluid displacement processes, *Fundamentals of Transport Phenomena in Porous Media*, Elsevier, Amsterdam, 229–240.

Sarma, H. K. and Bentsen, R. G. 1989a, A method for reducing model error when estimating relative permeabilities from displacement data, *J. Petrol. Sci. Engrg.* **2**, 331–347.

Sarma, H. K. and Bentsen, R. G., 1989b, A new method for estimating relative permeabilities from unstabilized displacement data, *J. Can. Petrol. Technol.* **28**(4), 118–128.

Sarma, H. K. and Bentsen, R. G., 1990, Further validation of the external-drive technique, *J. Can. Petrol. Technol.* **29**(4), 75–83.

Spanos, T. J. T., de la Cruz, V., Hube, J. and Sharma, R. C., 1986, An analysis of Buckley-Leverett theory, *J. Can. Petrol. Technol.* **25**(1), 71–75.

Spanos, T. J. T., de la Cruz, V. and Hube, J., 1988, An analysis of the theoretical foundations of relative permeability curves, *AOSTRA J. Res.* **4**, 181–192.

Spanos, T. J. T., de la Cruz, V. and Eastwood, J., 1991. Fluid flow in inhomogeneous porous media, paper No. 91–56 presented at the CIM/AOSTRA Technical Conference in Banff, Alberta.

Whitaker, S., 1986, Flow in porous media II: The governing equations for immiscible, two-phase flow, *Transport in Porous Media* **1**, 105–125.

Wooding, R. A. and Morel-Seytoux, H. J., 1976, Multiphase fluid flow through porous media, *Ann. Rev. Fluid Mech.* **8**, 233–274.